

# Validation of an efficient two-layer non-hydrostatic wave model on a sloping foreshore

Joost P. den Bieman<sup>1</sup>, Menno P. de Ridder<sup>2</sup>, and Madelief W. Doeleman<sup>3</sup>

## Abstract

In the physical modelling of coastal engineering problems, use is made of foreshores and transition slopes to obtain the desired wave conditions – both spectral parameters and wave height distribution – at a given location. Numerical models can be used to predict whether the target wave conditions are met for a given physical model layout and wave forcing. The XBeach non-hydrostatic two-layer model is a computationally efficient numerical model that has been validated for spectral wave parameters, but lacks validation of wave height distributions which are important when processes such as wave forces or wave run-up are of interest. In this work, wave flume data with high spatial density over a sloping foreshore is used to validate the ability of this numerical model to reproduce both spectral wave parameters and wave height distributions. This data contains offshore wave conditions with 1.0%, 2.5%, and 5.0% wave steepness. Optimal settings have been derived for the wave breaking in the numerical model, resulting in recommended values for *maxbrsteep* and *reformsteep* of 0.40 and 0.20 respectively.

From the results of the validation it is concluded that the numerical model is unsuccessful in reproducing the validation tests with 5.0% offshore wave steepness, potentially due to the associated higher  $k_p d$  numbers on the generating model boundary. Hence, using the numerical model with values of  $k_p d \geq 2$  on the model boundary is not recommended.

The XBeach non-hydrostatic two-layer model performs much better for the 1.0% and 2.5% offshore wave steepness tests, where the spectral wave parameters are represented well. The corresponding wave height distributions are represented reasonably well up to the point that the relative water depth gets very shallow. For shallower water, the model is expected to underestimate the higher waves. Additionally, the numerical model is shown to reproduce the wave height distribution better than a commonly used empirical formulation.

## Keywords:

Numerical modelling, XBeach, Physical modelling, Wave height distribution, Validation

## 1 Introduction

In the design of physical model experiments in coastal engineering, it is common that the construction of a foreshore is necessary to obtain the desired wave conditions at a given location – usually close to a structure being tested – and to allow for a large enough water depth at the wave board to be within the validity range of the wave theory used in wave generation. In addition to the commonly used spectral wave parameters to describe the target wave conditions, the wave height distribution and associated parameters (such

<sup>1</sup>[Joost.denBieman@deltares.nl](mailto:Joost.denBieman@deltares.nl); Deltares, Delft, The Netherlands

<sup>2</sup>[Menno.deRidder@deltares.nl](mailto:Menno.deRidder@deltares.nl); Deltares and TU Delft, Delft, The Netherlands

<sup>3</sup>[Madelief.Doeleman@deltares.nl](mailto:Madelief.Doeleman@deltares.nl); Deltares, Delft, The Netherlands

Research article. **Submitted:** 14 June 2024. **Reviewed:** 13 November 2024. **Accepted** after double-anonymous review: 27 November 2024. **Published:** 15 December 2024.

DOI: [10.59490/jchs.2024.0038](https://doi.org/10.59490/jchs.2024.0038)

Cite as: Den Bieman, J.P., De Ridder, M.P., Doeleman, M.W., Validation of an efficient two-layer non-hydrostatic wave model on a sloping foreshore, Journal of Coastal and Hydraulic Structures, 38, DOI: 10.59490/jchs.2024.0038

This paper is part of the **Thematic Series** of selected papers on advances in physical modelling and measurement of Coastal Engineering issues, as presented on the Coastlab Conference in Delft in 2024.



The Journal of Coastal and Hydraulic Structures is a community-based, free, and open access journal for the dissemination of high-quality knowledge on the engineering science of coastal and hydraulic structures. This paper has been written and reviewed with care. However, the authors and the journal do not accept any liability which might arise from use of its contents. Copyright © 2024 by the authors. This journal paper is published under a CC BY 4.0 license, which allows anyone to redistribute, mix and adapt, as long as credit is given to the authors.

as  $H_{max}$  and  $H_{2\%}$ ), wave periods and infra-gravity waves can be important to reproduce properly as well. Wave height distributions are typically important for tests where *e.g.* wave run-up or wave forces are of interest, as here the response is governed more by specific extreme waves instead of the mean characteristics of the wave spectrum (*e.g.* Jacobsen et al., 2018).

Some guidance on the design of foreshores is available in Frostick et al. (2011), which contains guidelines (in part based on experience) on transition slope angle and foreshore length after the transition slope. More recently, Eldrup and Lykke Andersen (2024) used numerical model results to derive guidelines for the water depth just after the transition slope. This water depth has to be large enough to prevent generation of unwanted free waves. Since the construction of foreshores and transition slopes is labour intensive (and thus expensive), it is useful to be able to check a priori (in addition to employing the existing guidelines) whether the target wave conditions are met with a given foreshore design and whether the chosen transition slope does not significantly influence the wave conditions. One way to do this is by using numerical wave models.

For a numerical model to be a useful design tool for physical model layouts, the predicted wave transformation (over the foreshore) needs to be sufficiently accurate. One option is to use computationally demanding models such as Boussinesq models or even very detailed CFD wave models for this purpose. CFD models such as OpenFOAM, which has been shown to accurately reproduce wave transformation (Higuera et al., 2013; Jacobsen et al., 2015, 2018), however, typically feature high computational demand that – in practice – often translates to computational times in the order of days for 2DV simulations. For full 3D simulations, this computational demand is even larger which means these simulations are hardly ever feasible in practice. This is a significant disadvantage in the context of designing a physical model experiment, the layout of which is often an iterative process which would be hampered by overly long computational times. Spectral wave models like SWAN (Booij et al., 1999), on the other hand, are much faster but do not model all the individual waves, rendering them unable to model wave height distributions. Empirical formulations for wave height distributions, such as the one for sloping bottoms by Battjes and Groenendijk (2000), are even quicker to assess, but are only valid for very simple geometries – as shown by Caires and van Gent (2012) – and require information regarding the local spectral wave height as an input parameter. Recent research has suggested changing the tail of the distribution (Wu et al., 2016) or fitting a new distribution (Karpadakis et al., 2022), but they do not change the limitations mentioned before. As a middle-ground, it seems that the XBeach model (Roelvink et al., 2009) used in its two-layer non-hydrostatic (XBeach-NH+) mode (de Ridder et al., 2021) – or other non-hydrostatic models such as SWASH (Zijlema et al., 2011) which has been shown to successfully model wave breaking behaviour (Roubos et al., 2021) – might present a workable compromise between computational time and accurate representation of the wave transformation. The XBeach-NH+ model has been validated by de Ridder et al. (2021) on bichromatic waves, complex barred beach geometry and a fringing reef for bulk wave parameters and spectral properties.

Expanding on earlier validation work, in this paper the ability of the XBeach-NH+ model to reproduce wave height distributions over a sloping foreshore is validated using high resolution wave flume data. This paper is structured as follows; Section 2 describes the physical model tests used as validation data. In Section 3, the numerical modelling is discussed, the results of which are expanded upon in Section 4. Section 5 contains a discussion and Section 6 formulates the conclusions of this work.

## 2 Physical model tests

### 2.1 Physical model setup

The physical model tests for the Sloping Foreshore (den Bieman et al., 2024) – or SloFor – experiments are performed in a wave flume facility with a length of 110 m, width of 1.0 m and height of 1.2 m. The wave board of this wave flume is equipped with Active Reflection Compensation and second-order wave generation. As is shown in Figure 1, the model setup features a 1:15 transition slope and horizontal step at 43.4 cm from the flume bottom, followed by a long 1:60 slope to a height of 71.7 cm from the flume bottom. The 1:60 slope is equipped with 15 wave gauges (manufactured in-house), capturing the wave transformation in a high spatial resolution (see Table 1).

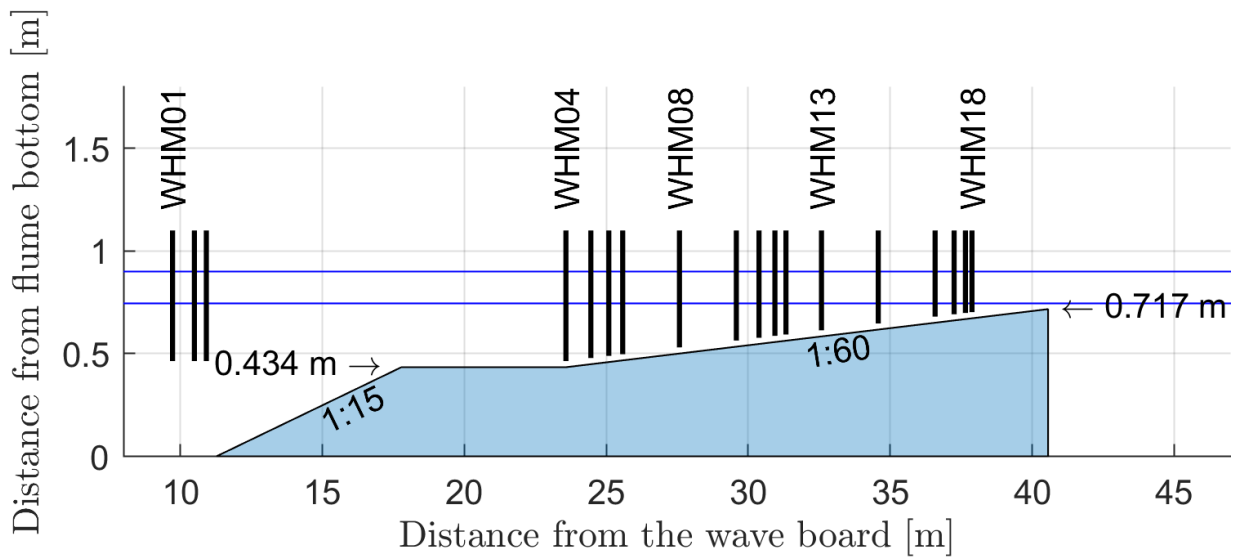


Figure 1| Setup of the SloFor physical model. The vertical lines mark the position of the wave gauges, the horizontal lines indicate the different water levels used in the test programme (see Table 2) and the blue area indicates the impermeable foreshore.

Table 1| Wave gauge locations in the physical model setup. Wave gauge location is defined as a distance from the wave board.

Wave gauge	Location [m]
WHM01	9.73
WHM02	10.50
WHM03	10.92
WHM04	23.58
WHM05	24.46
WHM06	25.09
WHM07	25.58
WHM08	27.58
WHM09	29.58
WHM10	30.38
WHM11	30.94
WHM12	31.33
WHM13	32.58
WHM14	34.58
WHM15	36.58
WHM16	37.25
WHM17	37.65
WHM18	37.88

## 2.2 Test programme

In the test program the wave steepness ( $s_{0p}$ ) at the offshore wave gauge array is varied between 1% and 5%, the relative water depth above the horizontal step ( $\frac{d_{step}}{H_{m0,In,deep}}$ ) is varied between 3.1 and 4.7 and the tests are performed with two different water depths. The incoming wave parameters are determined at the offshore wave gauge array using the de Ridder et al. (2023) modification of the Eldrup and Lykke Andersen (2019) nonlinear wave separation method. The test duration is aimed at about 1,000 waves, in order to ensure a proper representation of the wave spectrum. The data from the wave gauges is captured at a frequency of 40Hz.

Table 2| SloFor test programme with measured wave spectral parameters at the offshore wave gauge array. PM denotes a Pierson-Moskowitz wave spectrum.

Test	$d$ [m]	$H_{m0,In,deep}$ [m]	$T_{p,In,deep}$ [s]	$s_{0,p}$ [%]	Spectral shape	$k_p d$ [-]	$d_{step}/H_{m0,In,deep}$
D101	0.900	0.15	3.07	1.0	JONSWAP	0.7	3.1
D102	0.900	0.15	1.95	2.5	JONSWAP	1.2	3.1
D103	0.900	0.15	1.38	5.0	JONSWAP	2.0	3.1
D111	0.900	0.15	3.04	1.0	PM	0.7	3.1
D112	0.900	0.15	1.95	2.5	PM	1.2	3.1
D113	0.900	0.15	1.39	4.9	PM	2.0	3.1
D201	0.900	0.10	2.52	1.0	JONSWAP	0.8	4.7
D202	0.900	0.10	1.59	2.5	JONSWAP	1.6	4.7
D203	0.900	0.10	1.12	4.9	JONSWAP	2.9	4.7
D211	0.900	0.10	2.52	1.0	PM	0.8	4.7
D212	0.900	0.10	1.59	2.5	PM	1.6	4.7
D213	0.900	0.10	1.14	4.6	PM	2.8	4.7
L201	0.745	0.10	2.52	1.0	JONSWAP	0.7	3.1
L202	0.745	0.10	1.59	2.5	JONSWAP	1.4	3.1
L203	0.745	0.10	1.12	4.9	JONSWAP	2.4	3.1
L211	0.745	0.10	2.52	1.0	PM	0.7	3.1
L212	0.745	0.10	1.59	2.5	PM	1.4	3.1
L213	0.745	0.10	1.14	4.7	PM	2.4	3.1

## 3 Numerical modelling

### 3.1 The XBeach non-hydrostatic two-layer numerical model

The XBeach non-hydrostatic two-layer (XBeach-NH+) model, as described by de Ridder et al. (2021), is a phase-resolving non-linear implementation within the existing XBeach framework. It employs a two-layer approximation – as opposed to the earlier single layer implementation – to allow for better dispersive behaviour for higher  $kd$  numbers (up to about  $kd = 4$ , where  $k$  is the wave number and  $d$  is the water depth). The implemented two-layer approximation has two vertical layers, where the non-hydrostatic pressure is only included in the bottom layer. This approach provides a less computationally demanding alternative to full two-layer non-hydrostatic implementations. In the model simulations featured in this paper, the 'BOI-phase3' release of XBeach has been used (v1.24.5956).

In the XBeach-NH+ model, wave breaking is handled in a parameterized way by the so-called hydrostatic front approximation (Smit et al., 2013), which limits the upward velocity of the water surface to a fraction of the wave celerity (the *maxbrsteep* parameter). When this criterion is exceeded, wave breaking ensues and the cell is set to be hydrostatic. For neighbouring cells, the *reformsteep* criterion holds (again expressed as a fraction of the wave celerity, with *reformsteep* < *maxbrsteep*). In both cases, cells are back to non-hydrostatic as soon as the free surface moves downward again. Hence, wave breaking in the XBeach-NH+ model is controlled by the *maxbrsteep* and *reformsteep* parameters.

### 3.2 Numerical model schematization

The numerical model schematization uses a constant horizontal discretization of 0.02 m, which translates to between 100 and 750 points per wavelength depending on the wave period (based on  $L_{0,p}$ ). The wave flume is modelled in 1D, since it is assumed there is no significant variation over the width of the wave flume. The wave generating model boundary is located at the wave gauge closest to the wave board, where a *nonh\_1d* boundary type is applied. The model is forced by supplying the spectral parameters ( $H_{m0}$  and  $T_p$ ) of a JONSWAP or Pierson-Moskowitz spectrum, depending on the test. Using linear wave theory, the model converts the spectrum towards time series of velocity and surface elevation on the offshore boundary needed by the XBeach-NH+ solver. At the other side of the model, a 1D absorbing boundary is applied (boundary type *abs\_1d*). In the simulations, the CFL condition is set to a value of 0.55.

### 3.3 Validation approach

For the validation, the general idea is to force the numerical model with the same wave spectrum and water level as used in the physical model. Subsequently, the numerical model parameters to be tuned are the *maxbrsteep* and the *reformsteep* as described in Section 3.1. These two parameters essentially govern the start and ending of the parameterized wave breaking process in XBeach-NH+, and as such are expected to have a significant effect on both the spectral wave parameters and the wave height distribution. Values for these parameters from literature (Roelvink et al., 2018; de Ridder et al., 2021) are 0.4 and 0.6 (default value) for *maxbrsteep* and 0.25 for *reformsteep*. As mentioned in Section 3.1, these values represent a fraction of the wave celerity. Typical effects of varying the value of these parameters can be seen in Figure 2. This figure shows that the varying the *maxbrsteep* value mainly affects the amount wave height reduction of the highest waves, as expected. The effect is more pronounced for WHM15 where more wave breaking has already occurred. The variation in *maxbrsteep* value, however, seems to have very little effect in this case.

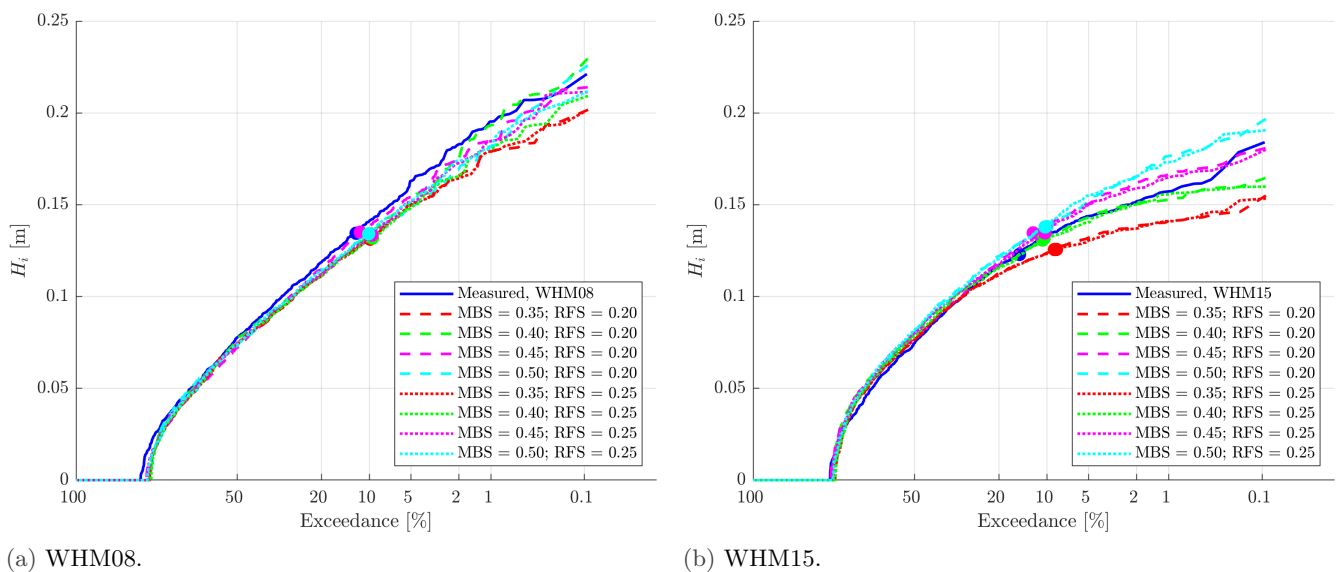


Figure 2 | Wave height exceedance distribution for WHM08 and WHM15 in test D103, with variations in the numerical model parameters related to wave breaking, where MBS and RFS refer to the *maxbrsteep* and *reformsteep* parameters respectively. The  $H_{m0}$  values are indicated with dots.

In the numerical model, the waves are specified as either a random JONSWAP or a random Pierson-Moskowitz spectrum, depending on the test. This is done instead of forcing the model with the exact wave train generated in the physical model. This choice is made with the intended use in mind, as a predictive simulation a-priori of a (potential) physical model test. In this case the exact realization of the wave train in a physical model is not known (yet).

From the results of the XBeach-NH+ model it becomes clear that, for many tests, the spectral wave height suddenly decreases slightly near the offshore model boundary, an example of which can be seen in Figure 3 in the top-left panel on the left-hand side. This appears to be a problem caused by the generating boundary, as it seems to be spatially confined to it. This behaviour seems analogous to what is commonly seen at wave boards in physical models, when the assumptions of the wave theory used to derive the wave steering do not (fully) hold for certain wave conditions. It is likely that in XBeach-NH+ a similar issue happens with the assumptions behind the *nonh\_1d* boundary condition used. In the figure, it can be seen that this problem affects the first one or two wave gauges, but WHM03 is unaffected. Hence, the choice was made to calibrate the wave forcing in the numerical model on WHM03, making sure that the  $H_{m0}$  at that wave gauge matches between the physical and numerical models. This in effect means calibrating the numerical model on the total spectral wave height instead of the just the incoming spectral wave height. The error because of this is expected to be small due to the small amount of wave reflection, given that this physical model setup features a long slope up to a very small water depth leading to much wave dissipation.

## 4 Results

### 4.1 Numerical model performance

As stated in Section 3.3, the performance of the XBeach-NH+ numerical model is evaluated on its ability to reproduce the spectral wave parameters ( $H_{m0}$  and  $T_{m-1,0}$ ) and the wave height distribution (represented by  $H_{10\%}$  and  $H_{2\%}$ ). Additionally, a comparison between maximum wave heights is also shown. The ability to reproduce the  $H_{max}$  is, however, not taken into account in the choice of recommended XBeach-NH+ parameter settings, since this parameter is known to be very sensitive to the exact wave train at the model boundary (which is also apparent in the right-hand side of the blue line in Figure 2). Since XBeach-NH+ is forced with a random realization from the spectrum, a deviation in  $H_{max}$  is to be expected.

Table 3| Mean absolute errors of the  $H_{m0}$ ,  $H_{10\%}$ ,  $H_{2\%}$  and  $H_{max}$  for WHM04 - WHM18. Listed values are for tests with  $k_p d < 2$ , values in brackets are for all tests listed in Table 2.

<i>maxbrsteep</i>	<i>reformsteep</i>	MAE $H_{m0}$ [%]	MAE $H_{10\%}$ [%]	MAE $H_{2\%}$ [%]	MAE $H_{max}$ [%]
0.35	0.20	2.5 (3.1)	5.1 (6.2)	9.2 (10.0)	14.8 (14.4)
0.35	0.25	2.5 (3.1)	5.2 (6.3)	9.3 (10.1)	14.9 (14.4)
0.40	0.20	2.7 (3.3)	3.7 (4.8)	6.3 (7.3)	10.7 (10.8)
0.40	0.25	2.7 (3.3)	3.7 (4.9)	6.4 (7.5)	10.4 (10.5)
0.45	0.20	3.7 (4.0)	3.2 (4.3)	4.6 (5.7)	7.5 (7.8)
0.45	0.25	3.7 (4.1)	3.4 (4.6)	4.2 (5.6)	8.0 (8.4)
0.50	0.20	5.0 (5.2)	3.8 (4.9)	3.6 (5.3)	6.8 (7.6)
0.50	0.25	5.1 (5.2)	3.9 (4.9)	3.5 (5.2)	6.8 (7.5)

Table 4| Relative bias of the  $H_{m0}$ ,  $H_{10\%}$ ,  $H_{2\%}$  and  $H_{max}$  for WHM04 - WHM18. Listed values are for tests with  $k_p d < 2$ , values in brackets are for all tests listed in Table 2.

<i>maxbrsteep</i>	<i>reformsteep</i>	Bias $H_{m0}$ [%]	Bias $H_{10\%}$ [%]	Bias $H_{2\%}$ [%]	Bias $H_{max}$ [%]
0.35	0.20	-0.1 (-1.4)	-3.7 (-5.3)	-9.2 (-10.0)	-14.0 (-13.8)
0.35	0.25	-0.2 (-1.5)	-3.8 (-5.4)	-9.2 (-10.1)	-14.0 (-13.9)
0.40	0.20	1.9 (0.5)	-1.1 (-2.9)	-6.0 (-7.0)	-9.4 (-9.6)
0.40	0.25	3.4 (1.9)	0.6 (-1.5)	-2.0 (-3.7)	-4.9 (-5.6)
0.45	0.20	4.9 (3.2)	2.3 (-0.2)	-1.1 (-3.1)	-1.4 (-2.5)
0.45	0.25	1.8 (0.4)	-1.3 (-3.3)	-6.1 (-7.3)	-9.1 (-9.6)
0.50	0.20	3.6 (2.0)	1.0 (-1.4)	-3.2 (-4.8)	-4.5 (-5.6)
0.50	0.25	5.0 (3.3)	2.7 (0.1)	-1.0 (-2.9)	-1.6 (-2.8)

Table 3 and Table 4 list the Mean Absolute Error (MAE, note that this includes the bias) and bias of the parameters mentioned above for different combinations of numerical model settings related to wave breaking. Note that the scores for both all tests and just the tests with  $k_p d < 2$  are listed, the latter of which is eventually used. The rationale behind this choice is explained in Section 4.2. The first pattern that emerges from Table 3 is that the difference in MAE between the *reformsteep* values of 0.20 and 0.25 is very small, which is consistent with the observations in Section 3.3. Even though the size of the errors is similar, the difference in bias (Table 4) is larger, where the former is more consistently underestimating and the latter sometimes overestimates as well.

Furthermore, Table 3 shows that the optimal value of *maxbrsteep* is different for  $H_{m0}$  (0.35),  $H_{10\%}$  (0.45) and  $H_{2\%}$  (0.50). Insight into why that is the case can be gained from Figure 3 and Table 4. The figure shows the spatial development of the wave height related parameters in the numerical and physical models. For the test shown in Figure 3, the  $H_{m0}$  matches quite well over the whole flume, while the  $H_{10\%}$  is slightly underestimated and in the  $H_{2\%}$  the underestimation is more pronounced (results corresponding with *maxbrsteep*=0.40). This pattern is consistent with the biases listed in Table 4, where the higher wave heights in the wave height distribution have a stronger tendency towards underestimation. A higher value of *maxbrsteep* effectively delays the breaking point, pushing the decline in  $H_{m0}$  shoreward (to the right in the figure). In smaller water depths, this will lead to overestimation of the  $H_{m0}$ . Consequently, this also increases the values for  $H_{10\%}$  and  $H_{2\%}$  compensating for their initial underestimation to some degree, which in turn leads to lower error scores. The focus in the validation is on the larger wave heights in the wave height distribution, since these are the most relevant for coastal engineering purposes. With the overestimation of for larger *maxbrsteep* values however, the wave height distribution as a whole also becomes worse due to the excess

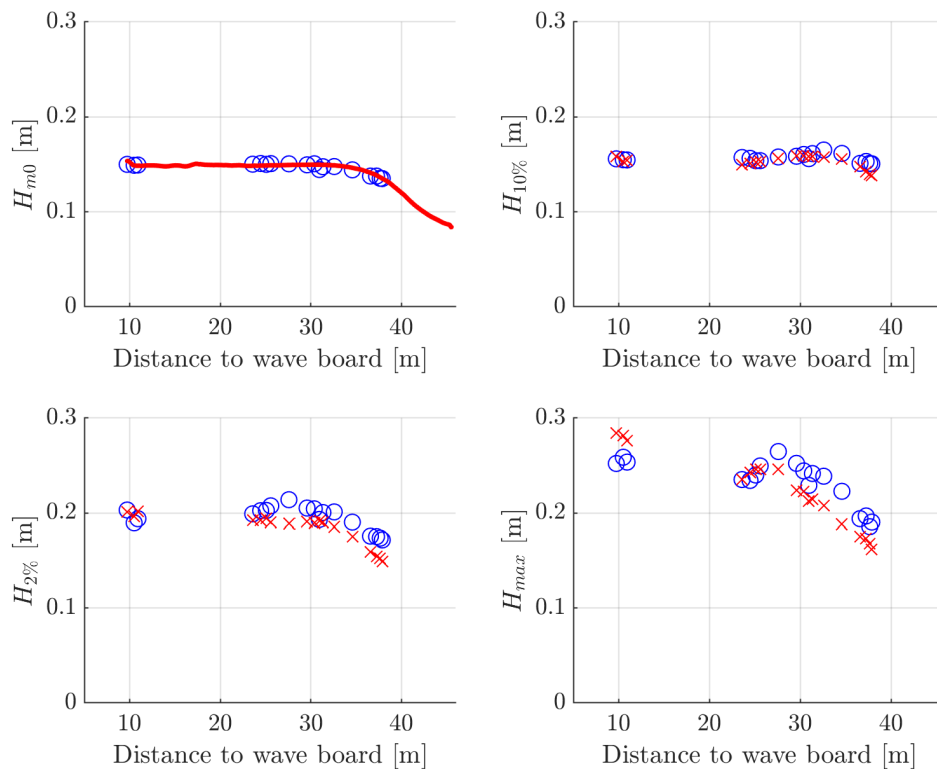


Figure 3| Example of spatial comparison of wave parameters between physical (blue) and numerical (red) models for Test D102, with  $maxbrsteep=0.40$  and  $reformsteep=0.20$ .

of wave energy simulated. In short, even though the error scores for  $H_{10\%}$  and  $H_{2\%}$  are lower for higher  $maxbrsteep$  values (0.45 and 0.50), these values are not to be recommended because they effectively overestimate the total amount of wave energy. Conversely, for smaller  $maxbrsteep$  values (0.35 and 0.40), the error in the  $H_{m0}$  is smallest and the errors for  $H_{10\%}$  and  $H_{2\%}$  are larger (both are generally underestimated). Based on the above, a  $maxbrsteep$  value of 0.4 is recommended, as the error for  $H_{m0}$  is only slightly larger than for a value of 0.35 while the errors for  $H_{10\%}$  and  $H_{2\%}$  are significantly smaller. This recommendation is based on the assumption that it is important to accurately reproduce the  $H_{m0}$  in addition to the wave height distribution, which is in practice often the case. For applications where only the small exceedance probabilities of the wave height distribution are important, better results might be obtained using  $maxbrsteep$  values of 0.45 or 0.50. As mentioned before, the results do not show convincing differences in MAE between  $reformsteep$  values of 0.20 and 0.25. In the rest of this paper, a value of 0.20 is used.

In addition to the comparison between the wave height distributions in the physical and numerical models, they are also compared to the empirical wave height distribution derived by Battjes and Groenendijk (2000). This is done by using the measured  $H_{m0}$  from the physical model as input and subsequently predicting the  $H_{10\%}$  and  $H_{2\%}$  for WHM04-WHM18 using Battjes and Groenendijk (2000) for all tests. Subsequently, the MAE is calculated w.r.t. the measured values for  $H_{10\%}$  and  $H_{2\%}$  to be able to compare with Table 3. Note that this assumes the ability to predict the  $H_{m0}$  with perfect accuracy, but in this way the assessment purely considers the accuracy of the Battjes-Groenendijk wave height distribution. This results in a MAE of 6.8% for the  $H_{10\%}$  and 7.3% for the  $H_{2\%}$ . Comparing this to the XBeach-NH+ results, it can be seen that the numerical model performs better with MAE values of 3.7% and 6.3% respectively. A potential reason as to why the empirical wave height distribution might perform worse is its shape. Battjes and Groenendijk (2000) prescribe a composite distribution with an abrupt transition at the transition wave height. In practice, the wave height distributions are transitioning more smoothly towards smaller gradients (as is demonstrated by the solid blue line in Figure 2). This is hypothesized to contribute to the slightly worse performance observed for the empirical Battjes and Groenendijk (2000) wave height distribution.

## 4.2 Influence of relative water depth

In Figure 4, the errors in the spectral wave parameters and the parameters related to wave height distribution are plotted against the relative water depth, defined as the local water depth normalized by the incoming offshore wave height ( $d/H_{m0,In,deep}$ ). The thing that stands out from the figure is the generally poor performance of the high wave

steepness conditions (red points), already in larger water depths. Note that in the calibration, the  $H_{m0}$  is made to very closely match the measured value on WHM03 (offshore wave gauge, not shown in the figure). So also for the higher wave steepness tests, the waves are properly entering the numerical model, but apparently the wave height has already been reduced too much by the time it reaches the start of the foreshore slope. It is hypothesized that the validity range mentioned in Section 3.1 (up to  $kd = 4$ ) holds for regular waves, but for irregular waves this criterion should in practice be more stringent. Even if  $k_p d < 4$  (based on peak wave period), the higher frequency part of the irregular wave spectrum might not completely adhere to  $kd = 4$  (for the  $k$  values associated with higher frequencies), leading to problems with the dispersive behaviour and wave propagation in the model. For now, the preliminary conclusion is that the XBeach-NH+ model is not suitable for wave conditions where  $k_p d \geq 2$  on the generating boundary. Consequently, the errors in Table 3 are presented both for all tests and excluding the tests where  $k_p d \geq 2$ .

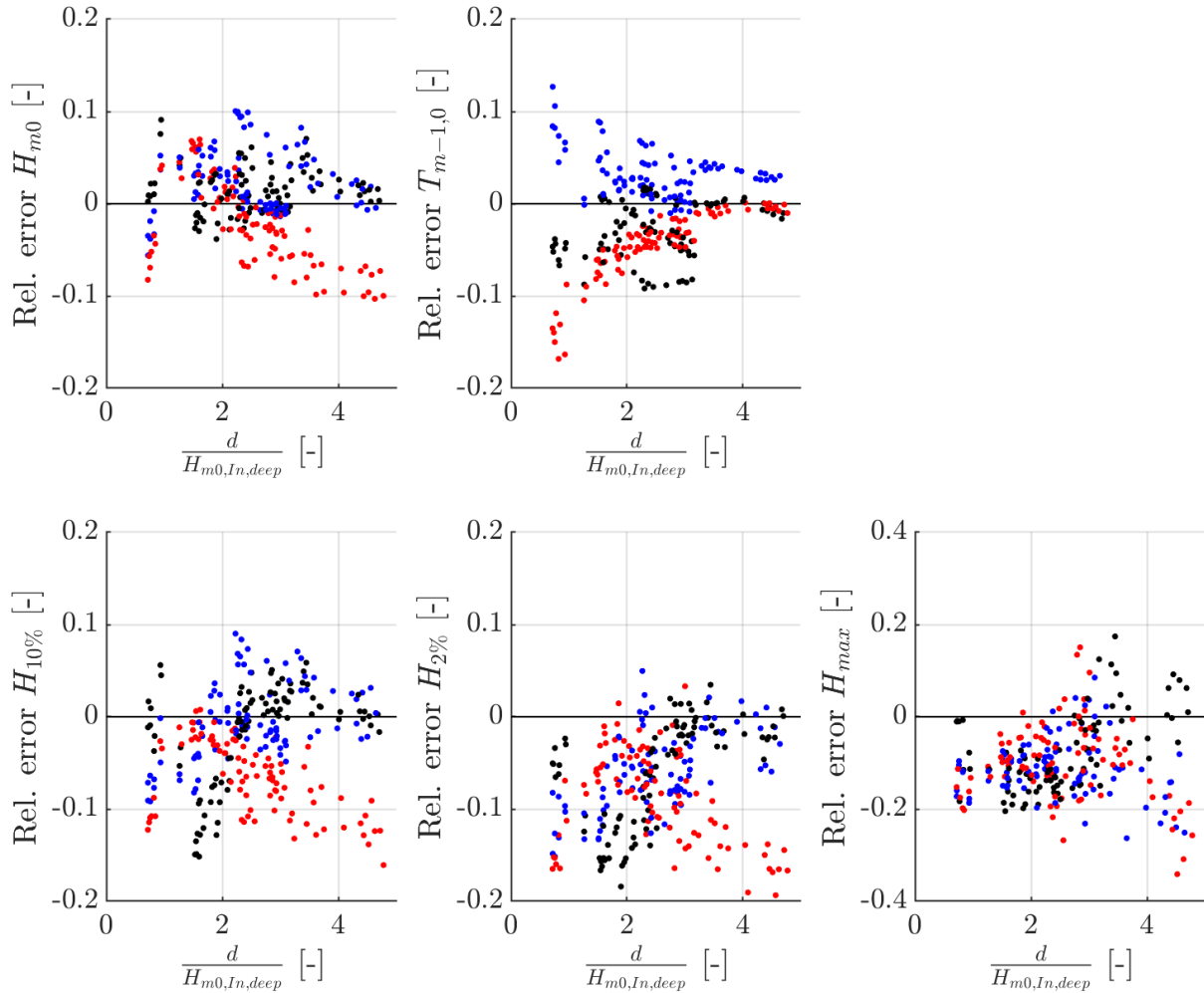


Figure 4| Relative errors plotted against relative depth for  $H_{m0}$ ,  $T_{m-1,0}$ ,  $H_{10\%}$ ,  $H_{2\%}$  and  $H_{max}$ . The colors indicate the different wave steepness with  $s_{0,p}$  around 1.0% (black), around 2.5% (blue) and around 5.0% (red). Note that limits of the vertical axis for the  $H_{max}$  (lower right panel) are larger than the other panels.

Regarding the wave conditions with lower steepness (black and blue dots in Figure 4), it can be seen that the accuracy of the model in reproducing the measurement data generally reduces for smaller relative water depths. This trend is more pronounced in the variables related to the wave height distribution ( $H_{10\%}$  and  $H_{2\%}$ ) than the spectral wave parameters. If, as an illustration, an absolute error margin of 10% is taken, then the error in  $H_{m0}$  stays below 10% for the entire depth range (down to  $d/H_{m0,In,deep} = 0.7$ ). The same is true for the  $T_{m-1,0}$ , with the exception of two data points in the upper left of the figure. For the  $H_{10\%}$ , errors are below 10% for  $d/H_{m0,In,deep} \geq 2.0$ , whereas for the  $H_{2\%}$  the depth needs to be larger ( $d/H_{m0,In,deep} \geq 2.6$ ). This also illustrates that the highest waves are harder to predict, and – looking at the trend – are generally underestimated by the model for smaller relative water depths. Note that the parameter ranges associated with the results presented above are a wave steepness ( $s_{0,p}$ ) between 1.0% and 2.5%, and a relative water depth on the sloping foreshore ( $d/H_{m0,In,deep}$ ) between 0.7 and 4.7.



## 5 Discussion

In Section 4.2 it is hypothesized that the poor XBeach-NH+ performance for the high wave steepness tests ( $s_{0,p}$  of around 5.0%) is due to the higher  $k_p d$  values associated with those conditions. Ideally, this hypothesis could be verified by additional validation data with similarly high wave steepness, but smaller  $k_p d$  values at the wave board (to the authors knowledge, this kind of validation data is currently not at hand). If XBeach-NH+ performs well for these conditions, this would support the hypothesis.

When examining the spatial patterns in the  $H_{m0}$  simulated by XBeach-NH+, a consistent sudden decline in  $H_{m0}$  is observed near the generating boundary (as mentioned in Section 3.3). While this phenomenon is more pronounced for the validation tests with higher values of  $k_p d$  and  $s_{0,p}$ , it is present in all of them. One explanation could be that this is inherent to the simplified nature of the two-layer approximation. This approximation does not perfectly match the natural velocity profile at the generating boundary, which is ‘corrected’ on a fairly small spatial scale. Regardless of the underlying cause, since the phenomenon is contained to the vicinity of the model boundary, a fairly easy way to cope with it is to calibrate for the desired wave conditions some distance from the model boundary (slightly landward of the sudden decline in  $H_{m0}$ ), an approach that is also applied in this work (Section 3.3). It is notable that Vasarmidis et al. (2024) encountered a very similar sudden decrease in wave height in the SWASH model (Zijlema et al., 2011), which they subsequently solved by a newly derived wave generation boundary. Perhaps a similar solution could also work in XBeach-NH+.

The validation results (Section 4.2) show that the ability of the model to reproduce the physical model tests reduces when the relative water depth ( $d/H_{m0,In,deep}$ ) becomes small. This effect seems stronger for the highest waves than for lower waves or the bulk wave height; *i.e.* the largest errors are found in  $H_{2\%}$ , then  $H_{10\%}$  and  $H_{m0}$  features the smallest errors. The first two are generally underestimated in relatively shallow water, while there is no clear trend in the error in  $H_{m0}$ . Comparing the simulated and measured wave height distributions in shallow water, it seems that the smaller waves are often slightly overestimated. This (partly) compensates the underestimation of the higher waves in calculating the  $H_{m0}$ , resulting in a smaller error there. Potentially, the shortcomings of the parameterized way of handling wave breaking in XBeach-NH+ are the cause of this, and these effects are naturally more pronounced in relatively shallow water as more wave breaking has been taking place. Additionally, a known fundamental difference between physical and numerical modelling is the setdown generated in the physical model due to wave-induced setup and water volume conservation that is absent in the numerical model (Gruwez et al., 2020). For the simulations presented in this paper, this effect is in the order of 1 mm and is expected not to significantly impact the conclusions presented here.

Given these results, foreshores and transition slopes in physical models could be optimized with aid of XBeach-NH+. For wave conditions adhering to the applicability limits of this work, a variety of potential foreshore designs – taking into account the guidelines on the design of foreshores – and hydrodynamic forcing conditions could be simulated in the design phase to assess whether target wave conditions are met at the desired location (usually near the toe of the structure to be tested). In interpreting the results one should be aware of the tendency towards the (earlier mentioned) underestimation of  $H_{10\%}$  and  $H_{2\%}$ , and the declining accuracy of the model in (very) shallow water described in Section 4.2. When the location of the target wave conditions is in relatively shallow water ( $d/H_{m0,In,deep} \leq 2.0 - 2.6$ ), significant underestimation of  $H_{10\%}$  and  $H_{2\%}$  of more than 10% is not uncommon. Note that it is recommended to verify that the target wave conditions in the physical model after the most optimal foreshore design has been constructed.

## 6 Conclusions

This work validates the ability of the numerical XBeach non-hydrostatic two-layer model to reproduce both spectral wave parameters and wave height distribution measured in a physical model containing a (very) shallow gently sloping foreshore. To this end, optimal settings for the parameterized wave breaking formulation in the model have been derived. For the *maxbrsteep* parameter, a value of 0.40 is recommended, while for the *reformsteep* parameter 0.20 is the recommended value (although it is good to note that the difference in performance with the value 0.25 found in literature is very small). In applications where accurate reproduction of  $H_{m0}$  is not important, and the focus is only on the small exceedance probabilities of the wave height distribution, better results might be obtained using *maxbrsteep* values of 0.45 or 0.50.

The numerical model showed poor performance for the cases with a high wave steepness (5.0%) at the offshore boundary, even for the spectral wave parameters. It is hypothesized that this is due to the higher  $k_p d$  numbers (2.0 - 2.9) on the generating model boundary for those validation tests. Until more clarity is reached on the cause of this

poor performance, it is recommended not to use the model for these high wave steepness values and/or  $k_p d \geq 2$ .

The numerical model performed much better for the 1.0% and 2.5% wave steepness tests, where the spectral wave parameters are represented well. The corresponding wave height distributions are represented reasonably well up to the point that the relative water depth gets very shallow. Mean absolute errors below 10% are found in case of relative water depths ( $d/H_{m0,In,deep}$ ) larger than 2.0 and 2.6 for  $H_{10\%}$  and  $H_{2\%}$  respectively. For shallower water, the model is expected to underestimate these wave heights. The model is shown to result in smaller errors for  $H_{10\%}$  and  $H_{2\%}$  than the empirical Battjes and Groenendijk (2000) formulation (with measured wave height as input) for the simple 1:60 validation slope, while also being able to simulate more complex nearshore bathymetries.

## Acknowledgements

The authors acknowledge that this work was partly funded by the Deltares SITO-IS Moonshot 2: Making the world safer from flooding.

## Author contributions (CRediT)

Den Bieman, J. P.: Conceptualization, Data curation, Formal Analysis, Investigation, Methodology, Visualization, Writing – original draft;

De Ridder, M. P.: Conceptualization, Investigation, Methodology, Writing – review & editing;

Doeleman, M. W.: Conceptualization, Methodology, Writing – review & editing.

## Data access statement

The SloFor wave flume data (den Bieman et al., 2024) used in this work is Open Access and available at [doi.org/10.4121/d2ac6c6f-bc13-4c80-ab68-c75550f11b3d](https://doi.org/10.4121/d2ac6c6f-bc13-4c80-ab68-c75550f11b3d)

## Declaration of interests

The authors report no conflict of interest.

## Notations

Table 5| List of symbols used in the paper.

Name	Symbol	Unit
Water depth	$d$	m
Water depth above the horizontal step	$d_{step}$	m
Spectral wave height	$H_{m0}$	m
Incoming spectral wave height decomposed at the offshore wave gauge array	$H_{m0,In,deep}$	m
10% exceedance wave height	$H_{10\%}$	m
2% exceedance wave height	$H_{2\%}$	m
Maximum wave height	$H_{max}$	m
Peak wave period	$T_p$	s
Incoming peak wave period decomposed at the offshore wave gauge array	$T_{p,In,deep}$	s
Spectral wave period	$T_{m-1,0}$	s
Deep water wave length based on $T_p$	$L_{0,p}$	-
Wave number	$k$	-
Wave number based on $T_p$	$k_p$	-
Wave steepness based on $L_{0,p}$	$s_{0,p}$	-

## Abbreviations

Table 6| List of abbreviations used in the paper.

Abbreviation	Meaning
XBeach-NH+	The XBeach non-hydrostatic two-layer numerical model
CFD	Computational Fluid Dynamics
SloFor	The Sloping Foreshore physical model experiments
MAE	Mean Absolute Error
WHM	Wave Height Meter (wave gauge)

## References

- Battjes, J.A. and Groenendijk, H.W. (2000). Wave height distributions on shallow foreshores. *Coastal Engineering*, **40**(3), 161–182. ISSN 0378-3839. DOI:[https://doi.org/10.1016/S0378-3839\(00\)00007-7](https://doi.org/10.1016/S0378-3839(00)00007-7).
- Booij, N., Ris, R.C. and Holthuijsen, L.H. (1999). A third-generation wave model for coastal regions: 1. model description and validation. *Journal of Geophysical Research: Oceans*, **104**(C4), 7649–7666. DOI:<https://doi.org/10.1029/98JC02622>.
- Caires, S. and van Gent, M.R.A. (2012). Wave height distribution in constant and finite depths. *Coastal Engineering Proceedings*, **1**(33). DOI:<https://doi.org/10.9753/icce.v33.waves.15>.
- de Ridder, M.P., Kramer, J., den Bieman, J.P. and Wenneker, I. (2023). Validation and practical application of nonlinear wave decomposition methods for irregular waves. *Coastal Engineering*, **183**, 104311. ISSN 0378-3839. DOI:<https://doi.org/10.1016/j.coastaleng.2023.104311>.
- de Ridder, M.P., Smit, P.B., van Dongeren, A.R., McCall, R.T., Nederhoff, K. and Reniers, A.J. (2021). Efficient two-layer non-hydrostatic wave model with accurate dispersive behaviour. *Coastal Engineering*, **164**, 103808. ISSN 0378-3839. DOI:<https://doi.org/10.1016/j.coastaleng.2020.103808>.
- den Bieman, J.P., de Ridder, M.P. and van der Werf, I. (2024). SloFor wave flume data. DOI:<https://doi.org/10.4121/d2ac6c6f-bc13-4c80-ab68-c75550f11b3d>.
- Eldrup, M.R. and Lykke Andersen, T. (2019). Estimation of Incident and Reflected Wave Trains in Highly Nonlinear Two-Dimensional Irregular Waves. *Journal of Waterway, Port, Coastal, and Ocean Engineering*, **145**(1), 04018038. ISSN 0733-950X. DOI:[https://doi.org/10.1061/\(ASCE\)WW.1943-5460.0000497](https://doi.org/10.1061/(ASCE)WW.1943-5460.0000497).
- Eldrup, M.R. and Lykke Andersen, T. (2024). Generation of highly nonlinear waves in a short wave flume, In: *Proceedings of CoastLab 2024: Physical Modelling in Coastal Engineering and Science*, DOI:<https://doi.org/10.59490/coastlab.2024.687>.
- Frostick, L.E., McLelland, S.J. and Mercer, T.G. (Editors) (2011). *Users Guide to Physical Modelling and Experimentation*, Experience of the HYDRALAB Network.
- Gruwez, V., Altomare, C., Suzuki, T., Streicher, M., Cappietti, L., Kortenhuis, A. and Troch, P. (2020). Validation of rans modelling for wave interactions with sea dikes on shallow foreshores using a large-scale experimental dataset. *Journal of Marine Science and Engineering*, **8**(9). ISSN 2077-1312. DOI:<https://doi.org/10.3390/jmse8090650>.
- Higuera, P., Lara, J.L. and Losada, I.J. (2013). Simulating coastal engineering processes with openfoam. *Coastal Engineering*, **71**, 119–134. ISSN 0378-3839. DOI:<https://doi.org/10.1016/j.coastaleng.2012.06.002>.
- Jacobsen, N.G., Van Gent, M.R.A., Capel, A. and Borsboom, M. (2018). Numerical prediction of integrated wave loads on crest walls on top of rubble mound structures. *Coastal Engineering*, **142**, 110 – 124. ISSN 0378-3839. DOI:<https://doi.org/10.1016/j.coastaleng.2018.10.004>.
- Jacobsen, N.G., van Gent, M.R. and Wolters, G. (2015). Numerical analysis of the interaction of irregular waves with two dimensional permeable coastal structures. *Coastal Engineering*, **102**, 13–29. ISSN 0378-3839. DOI:<https://doi.org/10.1016/j.coastaleng.2015.05.004>.
- Karmpadakis, I., Swan, C. and Christou, M. (2022). A new wave height distribution for intermediate and shallow water depths. *Coastal Engineering*, **175**, 104130. ISSN 0378-3839. DOI:<https://doi.org/10.1016/j.coastaleng.2022.104130>.

- Roelvink, D., McCall, R., Mehvar, S., Nederhoff, K. and Dastgheib, A. (2018). Improving predictions of swash dynamics in xbeach: The role of groupiness and incident-band runup. *Coastal Engineering*, **134**, 103–123. ISSN 0378-3839. DOI:<https://doi.org/10.1016/j.coastaleng.2017.07.004>. RISC-KIT: Resilience-increasing Strategies for Coasts Toolkit.
- Roelvink, J.A., Reniers, A.J.H.M., Van Dongeren, A.R., Van Thiel de Vries, J.S.M., McCall, R.T. and Lescinski, J. (2009). Modelling storm impacts on beaches, dunes and barrier islands. *Coastal Engineering*, **56**(11-12), 1133–1152. DOI:<https://doi.org/10.1016/j.coastaleng.2009.08.006>.
- Roubos, J., Glasbergen, T., Hofland, B., Bricker, J., Zijlema, M., Esteban, M. and Tissier, M. (2021). Formulation of a surf-similarity parameter to predict tsunami characteristics at the coast. *Journal of Coastal and Hydraulic Structures*, **1**. DOI:<https://doi.org/10.48438/jchs.2021.0009>.
- Smit, P., Zijlema, M. and Stelling, G. (2013). Depth-induced wave breaking in a non-hydrostatic, near-shore wave model. *Coastal Engineering*, **76**, 1–16. ISSN 0378-3839. DOI:<https://doi.org/10.1016/j.coastaleng.2013.01.008>.
- Vasarmidis, P., Klonaris, G., Zijlema, M., Stratigaki, V. and Troch, P. (2024). A study of the non-linear properties and wave generation of the multi-layer non-hydrostatic wave model swash. *Ocean Engineering*, **302**, 117633. ISSN 0029-8018. DOI:<https://doi.org/10.1016/j.oceaneng.2024.117633>.
- Wu, Y., Randell, D., Christou, M., Ewans, K. and Jonathan, P. (2016). On the distribution of wave height in shallow water. *Coastal Engineering*, **111**, 39–49. ISSN 0378-3839. DOI:<https://doi.org/10.1016/j.coastaleng.2016.01.015>.
- Zijlema, M., Stelling, G. and Smit, P. (2011). Swash: An operational public domain code for simulating wave fields and rapidly varied flows in coastal waters. *Coastal Engineering*, **58**(10), 992–1012. ISSN 0378-3839. DOI:<https://doi.org/10.1016/j.coastaleng.2011.05.015>.